THE JOURNAL OF PHYSICAL CHEMISTRY B

Article

pubs.acs.org/JPCB

Rotational Dynamics of Metal Azide Ion Pairs in Dimethylsulfoxide Solutions

Hyewon Son,[†] YoungAh Kwon,[†] Jinwoo Kim,[†] and Sungnam Park*[,†,‡]

[†]Department of Chemistry, Korea University, Seoul 136-701, Korea

[‡]Multidimensional Spectroscopy Laboratory, Korea Basic Science Institute, Seoul 136-713, Korea

Supporting Information

ABSTRACT: Azide ion is an excellent vibrational probe for studying ion−ion and ion−dipole interactions in solutions because its frequency is sensitively dependent on its local environments. When azide ion forms contact ion pairs with cations in dimethylsulfoxide (DMSO), free azide ion and contact ion pairs are spectrally well distinguished in FTIR spectra. Here, we investigated vibrational population relaxation, $P(t)$, and orientational relaxation dynamics, $r(t)$, of free azide ion and contact ion pairs (LiN_3, NaN_3, NH_4N_3, MgN_3^+, and CaN_3^+) in DMSO by IR pump−probe spectroscopy. For metal azide ion pairs, the metal ion slowed down the vibrational relaxation of azide ion by acting like a thermal insulator. Biexponential behavior of $r(t)$ was analyzed in the wobbling-in-a-cone model. The long time component of $r(t)$ of free azide ion was found to be viscosity-dependent. The wobbling motion of azide ion within the frame of metal azide ion pairs was weakly dependent on the countercation. When the overall orientational relaxation of metal azide ion pairs was analyzed by the extended Debye−Stokes−Einstein equation, it was well described under stick or superstick boundary conditions due to a strong interaction between the metal ion and DMSO molecules. Our experimental results provide important insight in understanding the rotational dynamics of small ionic species in polar solvents when the size of the ionic species is smaller than or comparable to that of the solvent molecule.

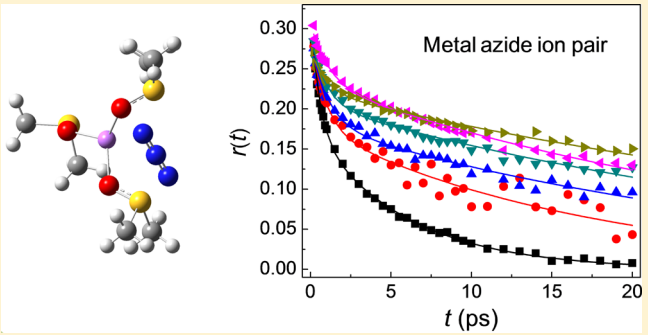

I. INTRODUCTION

Ion−ion (electrostatic) and ion−dipole interactions are ubiquitous and important in understanding the three-dimensional structures of proteins in aqueous ionic solutions,[1,2] ion pairing dynamics in electrolyte solutions,[3−5] ion clustering and transportations of charged species in polar solvents,[6,7] and rotational dynamics in ionic liquids.[8−10] Especially, for small ionic species whose size is smaller than or comparable to the solvent, such interactions play an important role in determining their dynamics. Since rotational dynamics are sensitively dependent on the interaction between the probing solute and its local environments, they can be utilized to understand the local intermolecular interactions.[7,11−13] In general, the rotating molecules in solutions experience either mechanical or dielectric friction depending on the nature of their interaction with the neighboring molecules.[14,15] The mechanical friction exists only when either the solute or the solvent is nonpolar or when both of them are nonpolar. Furthermore, the mechanical friction between the solute and the surrounding solvent depends on the size and shape of the solute molecule. When a polar solute undergoing rotational relaxation in a polar solvent polarizes the surrounding solvent medium and the response of the solvent polarization to the solute's rotation is not instantaneous, the rotating solute experiences the dielectric friction in addition to the mechanical friction. Dielectric friction depends fairly on the charge distribution and polarizability of the solute and the solvent molecules. In most cases, the mechanical and dielectric contributions to the friction are not separable.[14] The rotating solute experiences additional friction in the presence of specific interactions between the solute and the neighboring solvent, such as hydrogen-bonding or electrostatic interaction.[12,16−18] For small ionic species, the friction resulting from specific interactions plays dominant roles in determining the rotational dynamics.

Here, we investigated the rotational dynamics of azide ion and its contact ion pairs in dimethylsulfoxide (DMSO) by IR pump−probe (IR PP) spectroscopy and quantum chemical calculations. Azide ion (N_3^-) has a very strong infrared ν_3 band in the 2000−2100 cm^{-1} region and can be most conveniently used to characterize ion pairs and higher aggregates as well as intermolecular interactions including hydrogen-bonding and ion−dipole interaction. Chabanel and co-workers have studied azide ion pairs with alkali metals and alkaline earth metals in polar solvents by using FTIR spectroscopy and ab initio calculations.[19] They found that the ν_3 mode of N_3^- (azide ion) was very sensitive to the nature of metal ions and its frequency

Received: December 7, 2012
Revised: February 12, 2013
Published: February 14, 2013

shift for a given ion pair was linearly related to the polarizing power of metal ion. More recently, Owrutsky and co-workers have studied azide ion and metal azide ion pairs in polar solvents and reverse micelles.[20−23] They have investigated vibrational energy relaxation and rotational dynamics of metal azide ion pairs in DMSO by IR pump−probe experiments.[20] In their study, it was found that the vibrational lifetimes of azide ion pairs were slightly dependent on countercations and the rotational dynamics of azide ion pairs in DMSO were much slower than that of free azide ion. However, the rotational dynamics of azide ion pairs were not able to be analyzed in great detail due to the limited signal-to-noise ratio of their measurements.[20]

In this work, we have mainly focused on rotational dynamics of free azide ion and metal azide ion pairs in DMSO. When azide ion forms contact ion pairs with alkali or alkaline earth metals, rotational dynamics of metal azide ion pairs are significantly different from those of free azide ion. This results from a significant change in the interaction between the rotating species and neighboring solvent molecules. We found that the rotational dynamics were reasonably well fit by a biexponential function. Such biexponential behaviors were analyzed in the wobbling-in-a-cone model. The interaction between metal ion and azide ion was found to be relatively important in describing the wobbling motion of azide ion in contact ion pairs. The overall orientational diffusion of free azide ion and metal azide ion pairs was found to be viscosity-dependent and was described by the extended Debye−Stokes−Einstein equation. The overall orientational diffusion of metal azide ion pairs was dependent on the interaction between metal ion and DMSO molecules.

II. EXPERIMENTAL METHODS

A. Sample Preparation. Tetrabutyl ammonium azide (TBA-N_3), NH_4Cl, and metal halides (LiCl, NaBr, $MgCl_2$, and $CaCl_2$) were purchased from Sigma-Aldrich. 0.14 M N_3^- solution was prepared by directly dissolving TBA-N_3 in dimethylsulfoxide (DMSO). In DMSO, TBA-N_3 is fully dissociated into tetrabutyl ammonium and N_3^- ions. To prepare the metal azide ion pairs in DMSO, TBA-N_3 and halide salts are dissolved and the concentration of TBA-N_3 was 0.40 M and the concentrations of halide salts ([NH_4Cl] = 0.50 M, [LiCl] = 0.55 M, [NaBr] = 0.45 M, and [$CaCl_2$] = 0.30 M) were varied such that the absorbance of contact ion pairs was about 0.3−0.4. We found that the solubility of $MgCl_2$ salt was relatively low in DMSO. A sample solution with 0.25 M TBA-N_3 and saturated $MgCl_2$ was prepared for the MgN_3^+ ion pair in DMSO. The sample solutions were housed in a homemade IR cell with two 3 mm thick CaF_2 windows. The path length was set by a 12 μm (or 25 μm for $MgCl_2$) Teflon spacer. The viscosities of the sample solutions were measured by the Ostwald viscometer (SI Analytics GmbH, Germany) at 22 °C.

B. FTIR and IR Pump−Probe Spectroscopy. FTIR spectra of the sample solutions were measured by using a FTIR spectrometer (Varian 640-IR) with 1 cm^{-1} resolution. Before and after IR pump−probe experiments, the FTIR spectrum of each sample solution was measured to ensure that there was no significant change in the sample solution during IR pump−probe experiments. All experiments were carried out at 22 °C.

Our femtosecond laser system and IR pump−probe (IR PP) spectrometer have been described in detail elsewhere.[7,16] Briefly, a train of 800 nm pulses with ∼45 fs duration and ∼1.0 mJ per pulse was generated by a Ti:sapphire oscillator (Tsunami, Spectra-Physics) and regenerative amplifier (Spitfire, Spectra-Physics) laser system operating at 1 kHz. The 800 nm pulses were used to pump an optical parametric amplifier (OPA, Spectra-Physics) to produce near-IR pulses at ∼1.4 and ∼1.9 μm which were used to generate mid-IR pulses at 2050 cm^{-1} in a 0.5 mm thick $AgGaS_2$ crystal (type II) by difference frequency generation. The power spectrum of the mid-IR pulses had a Gaussian envelope with an ∼250 cm^{-1} bandwidth (full width at half-maximum). The CaF_2 plates with different thicknesses were used to compensate for the linear dispersion introduced by other dielectric materials in the setup including a Ge Brewster plate and ZnSe beam splitters. The mid-IR pulses were nearly transform-limited at the sample position.

In our IR PP experiments,[24,25] the IR pulses were split into the pump and probe beams with a 9:1 intensity ratio and were focused onto the sample. The probe beam was collimated after the sample and was dispersed through a spectrometer onto the 64-element MCT array detector. The IR PP signal $S(t)$ was collected by measuring the transmission of the probe beam through the sample by chopping the pump beam at 500 Hz. For a given delay time t, the IR PP signal was defined by $S(t) = [T_{\text{pump-on}} - T_{\text{pump-off}}](t)/T_{\text{pump-off}} = \Delta T(t)/T$, where T is the transmission of the probe beam. For polarization-controlled IR PP experiments, the wiregrid polarizers were placed in the pump and probe beam pathways before the sample and their polarization states were set to be 0 and 45° with respect to the normal to the optical table, respectively. A wiregrid analyzer polarizer on a motorized rotational stage was placed after the sample, and the parallel and perpendicular polarizations of the probe beam were selectively measured by setting the analyzer polarizer to be 0 and 90° by the computer-controlled motorized rotational stage. The parallel and perpendicular IR PP signals, $S_{\parallel}(\omega_{pr}, t)$ and $S_{\perp}(\omega_{pr}, t)$, were consecutively measured for every two scans with the polarization of the probe beam parallel and perpendicular to that of the pump beam, respectively.

III. RESULTS AND DISCUSSION

A. FTIR Study. Azide ion, N_3^-, is a linear molecular ion and has three spectrally distinct vibrational transitions: symmetric stretching vibration (ν_1 = ∼1320 cm^{-1}), asymmetric stretching vibration (ν_3 = ∼2000 cm^{-1}), and degenerate bending vibrations (ν_2 = ∼630 cm^{-1}). Figure 1 displays FTIR spectra of the asymmetric stretching band (ν_3) of free N_3^- ion and N_3^-

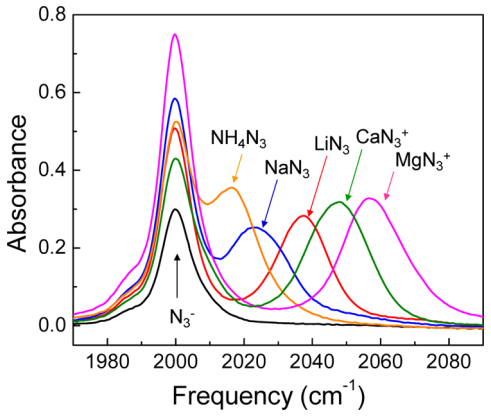

Figure 1. FTIR spectra of the asymmetric stretching mode (ν_3) of N_3^- in DMSO. The peak at 2000 cm^{-1} results from free azide ion, while the higher frequency peaks are from ion pairs. The frequencies of N_3^- in ion pairs were blue-shifted sensitively to the countercations.

dx.doi.org/10.1021/jp312055f | J. Phys. Chem. B 2013, 117, 2748−2756

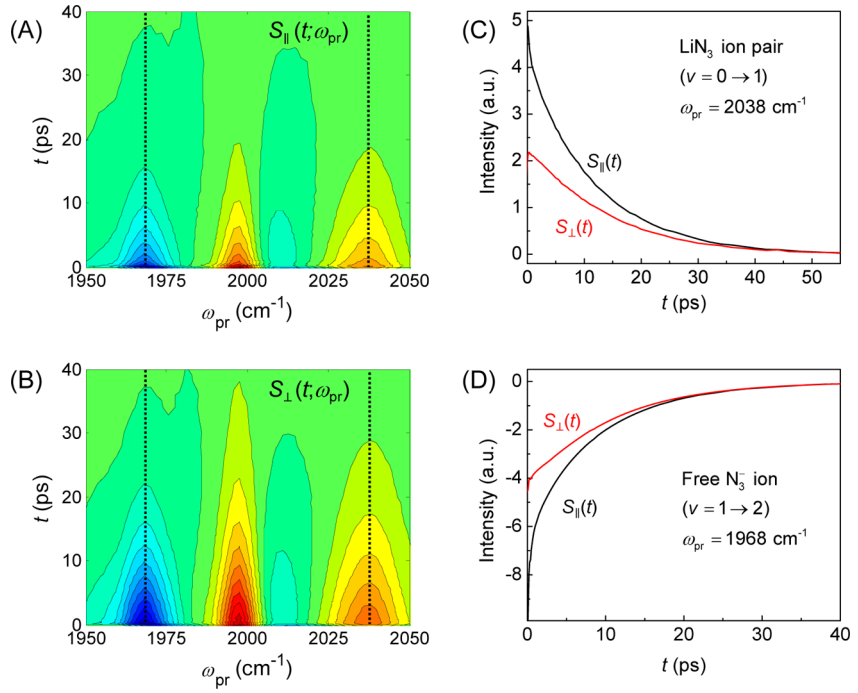

Figure 2. IR PP signals measured with Li^+ and N_3^- ions dissolved in DMSO. (A) Parallel, $S_{\parallel}(\omega_{pr}, t)$, and (B) perpendicular, $S_{\perp}(\omega_{pr}, t)$, frequency-resolved IR PP signals. (C) Parallel and perpendicular IR PP signals at ω_{pr} = 2038 cm^{-1} result from the $v = 0 \rightarrow 1$ transition of the LiN_3 ion pair. (D) Parallel and perpendicular IR PP signals at ω_{pr} = 1968 cm^{-1} result from the $v = 1 \rightarrow 2$ transition of free N_3^- ion.

Table 1. Exponential Fit to Vibrational Population Decay and Orientational Anisotropy Decay of Free Azide Ion and Ion Pairs in DMSO

	ω_{pr} (cm^{-1})	T_1 (ps)	a_1	τ_{or1} (ps)	a_2	τ_{or2} (ps)
N_3^-	2000	9.7 ± 0.5	0.15 ± 0.01	0.62 ± 0.03	0.17 ± 0.01	6.34 ± 1
LiN_3	2038	12.6 ± 0.5	0.084 ± 0.01	0.92 ± 0.1	0.21 ± 0.01	33.2 ± 2
NaN_3	2024	12.5 ± 0.5	0.097 ± 0.01	1.21 ± 0.1	0.18 ± 0.01	30.1 ± 2
MgN_3^+	2057	12.1 ± 0.5	0.070 ± 0.01	1.11 ± 0.2	0.23 ± 0.01	31.5 ± 2
CaN_3^+	2048	15.3 ± 0.5	0.062 ± 0.01	1.19 ± 0.2	0.21 ± 0.01	48.5 ± 2
NH_4N_3	2016	1.54 (0.8)[a] 8.16 (0.2)[a]	0.11 ± 0.02	0.90 ± 0.3	0.18 ± 0.01	16.9 ± 3

[a]Biexponential fit to $P(t)$ for the NH_4N_3 ion pair. The values in parentheses are the amplitudes.

in contact ion pairs in dimethylsulfoxide (DMSO). Examining the FTIR spectrum in Figure 1, the peak at ~2000 cm^{-1} results from free azide ion and its bandwidth (fwhm) is ~11 cm^{-1}. The peak position and width of azide ion are sensitively dependent on the local environments of azide ion. When azide ion (N_3^-) forms contact ion pairs ($MN_3^{(z-1)+}$) with alkali metal and alkaline earth metal ions (M^{z+}), the ν_3 mode of N_3^- is significantly blue-shifted and its bandwidth is increased. The frequency shift ($\Delta\nu$) of N_3^- in contact ion pairs is dependent on the countercation. In general, the frequency shift of a vibrational probe in solutions results from the vibrational solvatochromic effect.[26,27] The vibrational frequency of a solute in solutions is varied when the solute is placed in a different local electrostatic environment that is produced by the surrounding solvent molecules. Therefore, the frequency shift of a vibrational probe depends on the detailed solvation structure. Cho and co-workers have studied the vibrational solvatochromic effects with pseudohalide ions (CN^-, SCN^-, and N_3^-) in water, and they found that the vibrational frequencies of the pseudohalide ions are sensitively dependent on the hydrogen bond length and angle between water and such ions.[26] In the case of contact ion pairs in DMSO, the azide ion experiences a different local electrostatic field produced by both countercation and surrounding DMSO molecules. The frequency shift of azide ion in contact ion pairs is strongly influenced by the electrostatic interaction and relative geometry between the countercation and azide ion.

B. IR Pump–Probe Study. In IR pump–probe (IR PP) spectroscopy, a strong pump pulse excites a molecular system to the v = 1 state, and subsequently, the relaxation of the molecular system is monitored by the time-delayed probe pulse. In our IR PP experiments, the transmission of the probe beam is measured as a function of delay time (t) and furthermore the transmitted probe beam is frequency resolved to obtain the IR PP signal, $S(\omega_{pr}, t)$. Figure 2A and B display the parallel and perpendicular frequency-resolved IR PP signals, $S_{\parallel}(\omega_{pr}, t)$ and $S_{\perp}(\omega_{pr}, t)$, obtained with LiN_3 in DMSO solution. The frequency-resolved IR PP signals are contributed by the ground-state bleach (GSB, $v = 0 \rightarrow 1$) and stimulated emission (SE, $v = 1 \rightarrow 0$) or the excited-state absorption (ESA, $v = 1 \rightarrow 2$). In Figure 2A and B, GSB and SE contributions lead to an increase in the transmission of the probe beam (positive and red), while ESA contribution results in a decrease in the transmission of the probe beam (negative and blue). To

dx.doi.org/10.1021/jp312055f | J. Phys. Chem. B 2013, 117, 2748–2756

determine vibrational population relaxation and orientational relaxation dynamics, we analyzed IR PP signals at two probe frequencies: the $v = 0 \rightarrow 1$ transition for ion pairs and the $v = 1 \rightarrow 2$ transition for free azide ion because the $v = 0 \rightarrow 1$ transition (positive) of free azide ion was overlapped with the $v = 1 \rightarrow 2$ transition (negative) of ion pairs. For example, in the case of LiN_3 in DMSO, the parallel and perpendicular IR PP signals at $\omega_{pr} = 2038\ cm^{-1}$ ($v = 0 \rightarrow 1$) for the LiN_3 contact ion pair and $\omega_{pr} = 1968\ cm^{-1}$ ($v = 1 \rightarrow 2$) for the free azide ion were used, as shown in Figure 2C and D, respectively. They are indicated as dotted lines in Figure 2A and B. The corresponding $v = 0 \rightarrow 1$ transition frequencies for free azide ion and ion pairs are denoted as ω_{pr} in Table 1. Vibrational population decay, $P(t)$, and orientational anisotropy decay, $r(t)$, are determined from $S_{\parallel}(\omega_{pr}, t)$ and $S_{\perp}(\omega_{pr}, t)$ at a given probe frequency[16,25]

$$P(t) = S_{\parallel}(t) + 2S_{\perp}(t) \quad (1)$$

$$r(t) = \frac{S_{\parallel}(t) - S_{\perp}(t)}{S_{\parallel}(t) + 2S_{\perp}(t)} = \frac{2}{5}C_2(t) \quad (2)$$

where $C_2(t)$ is the orientational correlation function and is represented by the second-order Legendre polynomial of the transition dipole correlation function, $C_2(t) = \langle P_2[\boldsymbol{\mu}(t)\cdot\boldsymbol{\mu}(0)]\rangle$.

C. Vibrational Population Relaxation Dynamics. Vibrational relaxation of a given mode in a polyatomic molecule in solutions requires the initially excited mode to dissipate its energy to lower frequency intramolecular vibrations and intermolecular modes such as solvent bath modes.[28] The rate of vibrational relaxation depends on the molecular coupling of the initially excited mode to the accepting modes and the density of states of the accepting modes.[28] Vibrational population relaxation dynamics of small ions were sensitively varied in different polar solvents.[12,29,30] Figure 3A shows $P(t)$ of free N_3^- ion and contact ion pairs measured at the $v = 0 \rightarrow 1$ transition whose frequencies are given in Table 1. $P(t)$ is directly proportional to the population of the vibrationally excited molecules at a given delay time (t). Therefore, $P(t)$ is well described by a first-order kinetic process and is fit by a single exponential function

$$P(t) = A\ \exp(-t/T_1) \quad (3)$$

where T_1 is the vibrational lifetime. The fit results for free azide ion and ion pairs are summarized in Table 1. ω_{pr} in Table 1 represents the $v = 0 \rightarrow 1$ transition frequency for a given salt solution. The vibrational lifetime of the ν_3 mode of free N_3^- ion obtained in our experiments is $T_1 = 9.7 \pm 0.5$ ps and is in excellent agreement with the results of Owrutsky and co-worker ($T_1 = 11 \pm 2$ ps).[20] As shown in Figure 3A, $P(t)$ is dependent on the countercations in contact ion pairs. The vibrational lifetimes of the ν_3 mode are relatively longer in metal azide ion pairs than in free azide ion. In metal azide ion pairs, the vibrational energy dissipation of the excited ν_3 mode of N_3^- to the neighboring solvent bath modes becomes less favorable because the bound metal ion behaves like a thermal insulator blocking the relaxation pathway to the solvent bath.[12] On the other hand, $P(t)$ of the NH_4N_3 contact ion pair is much faster than that of free azide ion and is well fit by a biexponential function. In the case of the NH_4N_3 ion pair, NH_4^+ is hydrogen-bonded to N_3^- ion. The intramolecular vibrational modes of NH_4^+ can provide additional intermolecular energy dissipation pathways. The NH bending mode

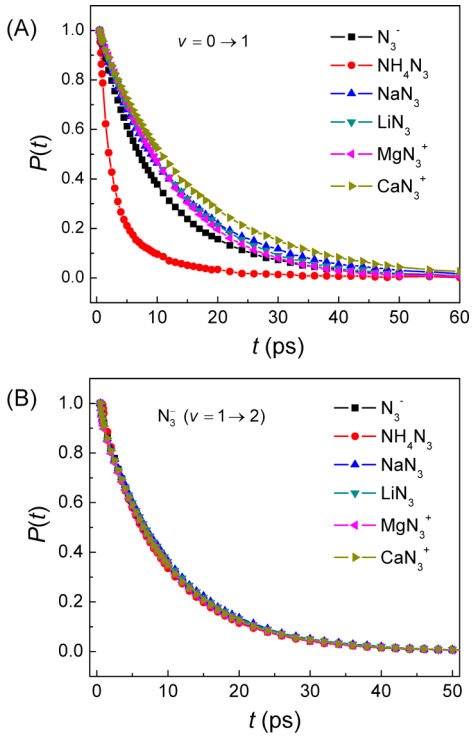

Figure 3. (A) Vibrational population decays, $P(t)$, of N_3^-, NH_4N_3, and metal azide ion pairs measured at the $v = 0 \rightarrow 1$ transition of which the corresponding frequency is shown in Table 1. (B) Vibrational population decays of free N_3^- ions measured at the $v = 1 \rightarrow 2$ transition are almost identical within our experimental error.

and combination modes seem to play an important role in the vibrational relaxation of N_3^- ion.

Figure 3B displays $P(t)$ of free azide ions in different salt solutions that are shown to be independent of salt solutions. It should be emphasized again that we analyzed $P(t)$ of free azide ions measured at $\omega_{pr} = \sim 1968\ cm^{-1}$ ($v = 1 \rightarrow 2$ transition) because the fundamental transition ($v = 0 \rightarrow 1$) of free azide ions was overlapped with the $v = 1 \rightarrow 2$ transition of metal azide ion pairs. In the TBA-N_3 solution where only free azide ions exist, we found that both $P(t)$ and $r(t)$ measured for the $v = 0 \rightarrow 1$ and $v = 1 \rightarrow 2$ transitions were almost identical within our experimental error, implying that the dynamics of free azide ion measured at the $v = 0 \rightarrow 1$ and $v = 1 \rightarrow 2$ transitions are indistinguishable (see Figure S2 in the Supporting Information).

D. Orientational Relaxation Dynamics. In IR PP experiments, the linearly polarized pump pulse excites the molecular system and the molecules with their transition dipoles parallel to the polarization of the pump pulse are vibrationally excited.[25] The transition dipoles of excited molecules are randomized as the excited molecules undergo orientational relaxation. Therefore, the IR PP signal includes information on rotational dynamics of the probing molecule. Figures 4A and 5A display $r(t)$ of free azide ions and contact ion pairs, respectively. In fact, $r(t)$ has a theoretical maximum value of 0.4 at $t = 0$ ps. However, the values of experimentally determined $r(t = 0)$ in Figures 4A and 5A are less than 0.4.[25,31] This results from the fact that the initial inertial orientation anisotropy decays of the probing molecules were not able to be fully resolved in our experiments. $r(t)$ of free azide ion and contact ion pairs was well fit by a biexponential function

dx.doi.org/10.1021/jp312055f | J. Phys. Chem. B 2013, 117, 2748−2756

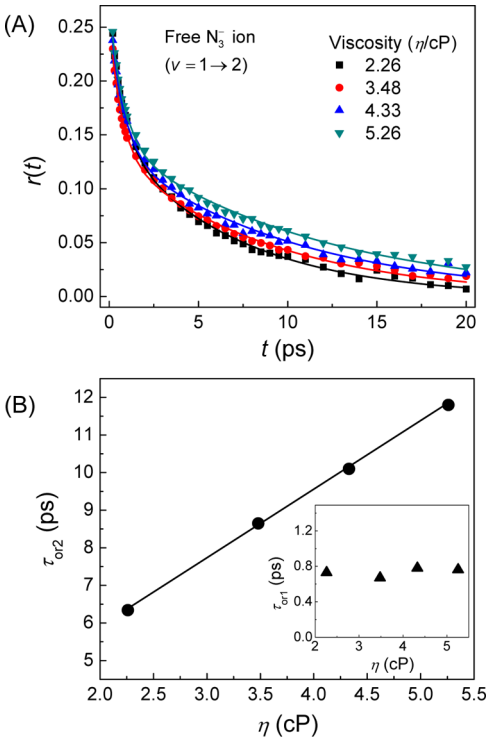

Figure 4. (A) Orientational anisotropy decays, $r(t)$, of free N_3^- ions measured at the $v = 1 \rightarrow 2$ transition. (B) Plot of τ_{or2} against the solution viscosity (η). The inset shows the plot of τ_{or1} against η. τ_{or2} is linearly increased with increasing η, while τ_{or1} is independent of η. Here, η was measured with each solution and summarize in Table 3.

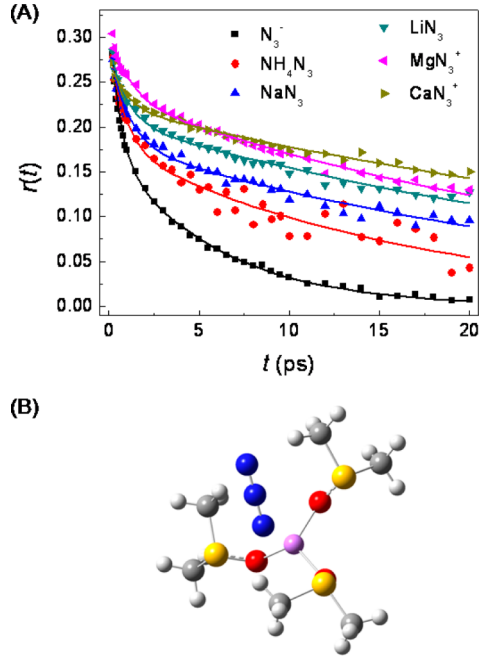

Figure 5. (A) Orientational anisotropy decays, $r(t)$, of N_3^-, NH_4N_3, and metal azide ion pairs measured at the $v = 0 \rightarrow 1$ transition. (B) Optimized structure of a LiN_3 ion pair with three DMSO molecules obtained by the quantum chemical calculation. Li^+ ion is not along the molecular axis of the azide ion. The oxygen atoms of DMSO molecules appear to be bound with Li^+ ion.

$$r(t) = a_1 \exp(-t/\tau_{or1}) + a_2 \exp(-t/\tau_{or2}) \quad (4)$$

where $\tau_{or1} < \tau_{or2}$. The biexponential fit result is summarized in Table 1.

For free azide ions, $r(t)$ measured at the $v = 1 \rightarrow 2$ transition was analyzed because the $v = 0 \rightarrow 1$ transition of free azide ions was significantly overlapped with the $v = 1 \rightarrow 2$ transition of contact ion pairs. The short time component (τ_{or1}) and the long time component (τ_{or2}) of $r(t)$ of free azide ions were found to have comparable amplitudes contributing similarly to $r(t)$ (i.e., $a_1 \approx a_2$). As shown in Figure 4, τ_{or2} was linearly increased by the solution viscosity (η), while τ_{or1} was independent of the solution viscosity. This is an interesting observation. Because N_3^- ion is smaller than DMSO, the orientational diffusion of N_3^- ion should be mainly influenced by local N_3^-–DMSO interactions but not by the solution viscosity which is a bulk property. In this case, it can be interpreted that the orientational diffusion of N_3^- ion at short times is a restricted orientational motion that is dictated by the local N_3^-–DMSO interaction and is independent of the solution viscosity. In contrast, the long time component of $r(t)$ results from the overall orientational diffusion of N_3^- ions without a restriction of the local N_3^-–DMSO interaction and thus is dependent on the solution viscosity and is presumably described by the hydrodynamic theory, which will be discussed later.

In Figure 5A, $r(t)$ of metal azide ion pairs is found to be substantially dependent on the countercations. When the amplitudes (a_1 and a_2) of two decaying components (τ_{or1} and τ_{or2}) are compared in Table 1, the long time component (τ_{or2}) contributes mainly to $r(t)$ for metal azide ion pairs. The biexponential behavior of $r(t)$ of contact ion pairs was found to be well described by a restricted orientational diffusion.[12] The orientational diffusion of N_3^- ion in the metal azide ion pair is restricted at short times by an electrostatic interaction between metal ion and azide ion. The long time component is associated with the overall orientational relaxation of the metal azide ion pair.

Before this section is closed, it is worthwhile noting that the rotational dynamics of free N_3^- ion, NaN_3, MgN_3^+, and CaN_3^+ ion pairs in DMSO were measured earlier by Owrutsky and co-worker.[20] They studied the orientational anisotropy decays by the IR PP method and found that the orientational anisotropy decay of free azide ion was much slower than that of metal azide ion pairs. However, the signal-to-noise (S/N) ratios of their measurements seem to limit detailed analyses of the orientational anisotropy decays. In contrast, the greatly enhanced S/N ratios of our measurements allow us to make detailed analyses of $r(t)$ which will be presented below.

D-1. Wobbling-in-a-Cone Model Analysis. In the context of a restricted orientational relaxation, the biexponential behaviors of $r(t)$ of free azide ion and metal azide ion pairs can be analyzed within a wobbling-in-a-cone model.[12,16,24,25,32,33] In this model, two independent orientational diffusion processes are occurring at the same time. The short time component is associated with the wobbling motion of a restricted rotor, whereby the transition dipoles undergo orientational diffusion within a cone of semiangle θ_c. The long time component accounts for the slower overall orientational relaxation without any angular restriction that leads to complete orientational randomization. In the wobbling-in-a-cone model, the orientational correlation function, $C_2(t)$, is expressed by[33,34]

dx.doi.org/10.1021/jp312055f | J. Phys. Chem. B 2013, 117, 2748–2756

$$C_2(t) = [Q^2 + (1 - Q^2)\exp(-t/\tau_w)]\exp(-t/\tau_l) = \frac{5}{2}r(t) \quad (5)$$

where Q^2 ($0 \le Q^2 \le 1$) is the generalized order parameter that describes the degree of restriction on the wobbling-in-a-cone orientational motion. Here, $Q^2 = 0$ represents unrestricted orientational motion, while there is no wobbling-in-a-cone orientational motion when $Q^2 = 1$. τ_w is the time constant that describes the wobbling motion. The time constant of the final full diffusive orientational motion is denoted τ_l, which is equal to the long time constant in eq 4, $\tau_l = \tau_{or2}$. τ_l is directly associated with the orientational diffusion constant, $D_l = 1/6\tau_l$, which results from the relation between the decay of the second Legendre polynomial and the orientational diffusion constant. τ_w is obtained from the experimentally measured τ_{or1} and τ_{or2} using the relation $\tau_w = (\tau_{or1}^{-1} - \tau_{or2}^{-1})^{-1}$. The cone semiangle ($\theta_c$) is determined from the order parameter $Q = [0.5\cos\theta_c(1 + \cos\theta_c)]$. The wobbling-in-a-cone diffusion constant D_w is calculated by[33,34]

$$D_w = \frac{x_w^2(1 + x_w)^2\{\ln[(1 + x_w)/2] + (1 - x_w)/2\}}{\tau_w(1 - Q^2)[2(x_w - 1)]} + \frac{(1 - x_w)(6 + 8x_w - x_w^2 - 12x_w^3 - 7x_w^4)}{24\tau_w(1 - Q^2)} \quad (6)$$

where $x_w = \cos\theta_c$. In the limit of $\theta_c = 180°$, there is no restriction to the orientational diffusion and $Q^2 = 0$ and $D_w = 1/6\tau_w$.

Table 2 summarizes the parameters obtained from the wobbling-in-a-cone model analysis. The cone semiangles (θ_c) and wobbling time constants (τ_w) for metal azide ion pairs appear to be slightly influenced by the metal ions. θ_c is smaller and τ_w is shorter for cations with higher charge density (Li^+ vs Na^+ and Mg^{2+} vs Ca^{2+}) in the same group. This result suggests that the electrostatic interaction between metal ion and azide ion should be relatively important in the wobbling orientational diffusion of azide ion in metal azide ion pairs. For example, azide ion undergoes wobbling orientational diffusion with a larger cone semiangle and longer wobbling time constant in the NaN_3 ion pair than the LiN_3 ion pair because N_3^- ion is more weakly bound to Na^+ ion than Li^+ ion. In the case of the NH_4N_3 ion pair, N_3^- ion is hydrogen-bonded to ammonium ion (NH_4^+) and the wobbling orientational diffusion of N_3^- ion in the NH_4N_3 ion pair is not so much different from that in metal azide ion pairs.

Table 2. Cone Semiangle and Orientational Diffusion Coefficients

	Q	θ_c (deg)	τ_w (ps)	τ_l (ps)	D_w^{-1} (ps)	D_l^{-1} (ps)
N_3^-	0.43	42	0.69	6.34	5.32	38.0
LiN_3	0.53	37	0.95	33.2	9.13	199
NaN_3	0.45	40	1.26	30.1	10.3	181
MgN_3^+	0.58	34	1.15	31.5	12.6	189
CaN_3^+	0.53	36	1.22	48.5	11.8	291
NH_4N_3	0.45	40	0.95	16.9	7.75	101

The overall orientational diffusion (τ_l) of metal azide ion pairs is found to be more significantly dependent on the countercations. Within the framework of the Debye–Stokes–Einstein (DSE) equation, the orientational diffusion of a molecule is sensitively dependent on the solution viscosity. In the case of free azide ions, τ_l ($=\tau_{or2}$) is found to be linearly dependent to the solution viscosity (η), as shown in Figure 4. In a similar way, the overall orientational diffusion (τ_l) of metal azide ion pairs can also be assumed to be viscosity-dependent based on the wobbling-in-a-cone model.

D-2. Extended Debye–Stokes–Einstein (DSE) Equation. The long time component ($\tau_{or2} = \tau_l$) of $r(t)$ of metal azide ion pairs can be described by the extended Debye–Stokes–Einstein (DSE) equation

$$\tau_{rot} = \frac{1}{6D_{rot}} = \frac{\eta VfC}{k_B T} \quad (7)$$

where k_B and T are the Boltzmann constant and the temperature, respectively, and V is the van der Waals volume of a solute. f is the shape factor introduced by Perrin[35] to account for the nonspherical shape of the solute, and C is the friction coefficient that determines the extent of coupling between the solute and the neighboring solvents.[36] For a given molecule, the friction coefficient (C) contains information on the rotational friction experienced by the molecule. When the size of the rotating molecule is much larger than that of the solvent molecules, the friction coefficient is $C_{stick} = 1$, which represents the stick boundary condition. Under the stick boundary condition, it is assumed that the solvent molecules in the first solvation layer stick to the solute and thus there is no relative velocity between them. However, the rotating molecule is of comparable size or smaller than the solvent molecule and the friction coefficient is in the range $0 < C_{slip} < 1$, which is known as slip boundary condition. Using the dimension of a rotating molecule, the shape factors (f) and theoretical slip friction coefficients (C_{slip}) can be calculated from the tables of Hu and Zwanzig[36] and are shown in Table 3. If the solution viscosity (η) and temperature are further known, the rotational time constants (denoted τ_{rot}^{stick} and τ_{rot}^{slip}, respectively) of a solute under stick and slip boundary conditions can be readily calculated from eq 7. For metal azide ion pairs, the

Table 3. Rotational Time Constants Calculated from the Extended DSE Equation and the Parameters Used in the Extended DSE Equation

	η^a (cP)	V^b (Å^3)	f	C_{slip}	τ_{rot}^{slip} (ps)	$\tau_{rot}^{stick\ c}$ (ps)	τ_l (ps)	$\tau_l/\tau_{rot}^{stick}$
N_3^-	2.26	4.00	2.73	0.406	2.52	6.19	6.34	1.02
LiN_3	5.21	4.87	3.64	0.546	12.6	23.0	33.2	1.44
NaN_3	4.33	8.07	4.25	0.609	22.3	36.6	30.1	0.82
MgN_3^+	3.48	4.50	3.48	0.527	7.07	13.4	31.5	2.35
CaN_3^+	5.26	8.20	4.27	0.611	22.7	45.4	48.5	1.07

[a]The viscosity of each solution was measured with an Ostwald viscometer. [b]The radii of cations used here for the calculations was from Chapter 1 in ref 38. [c]$C_{stick} = 1$ is used for all the calculations of τ_{rot}^{stick}.

dx.doi.org/10.1021/jp312055f | J. Phys. Chem. B 2013, 117, 2748–2756

Table 4. Results of Quantum Chemical Calculations of Metal Azide Ion Pairs in DMSO

	asym. N_3^- [a] (cm^{-1})	str. $M^{z+}-N_3^-$ [a] (cm^{-1})	d ($M^{z+}-N_3^-$) (Å)	d ($M^{z+}-O$) (Å)	θ ($M^{z+}-N-N$) (deg)
LiN_3	2044	396	2.07	1.96	126
NaN_3	2032	219	2.40	2.27	120
MgN_3^+	2111	442	2.02	1.97	131
CaN_3^+	2090	335	2.27	2.25	137

[a]Frequency correction is made by the vibrational scaling factor (0.96) for the DFT method and basis set used for the calculation.

experimentally measured values of τ_l are compared with the rotational time constants (τ_{rot}^{stick} and τ_{rot}^{slip}) calculated from the extended DSE equation in Table 3. For free azide ion and CaN_3^+ ion pair, τ_l is almost identical to τ_{rot}^{stick}. For LiN_3 and MgN_3^+ ion pairs, τ_l is substantially larger than τ_{rot}^{stick}, which is known as a superstick boundary condition suggesting that the contact ion pairs have strong interactions with the neighboring solvent molecules. In other words, DMSO molecules are strongly bound to the metal ion by ion−dipole interactions and the orientational diffusion of LiN_3 and MgN_3^+ ion pairs significantly slows down. When two cations in the same group in the periodic table are compared (Li^+ vs Na^+ and Mg^{2+} vs Ca^{2+}), the ratio of $\tau_l/\tau_{rot}^{stick}$ is much larger for the smaller cation, which has a larger charge density. The same trend is also found for the wobbling motion of azide ion in contact ion pairs. This results from the fact that the metal ions with higher charge density are strongly bound with both the counteranions and dipolar solvent molecules.

E. Quantum Chemical Calculations. To understand the structures of metal azide ion pairs in DMSO, quantum chemical calculations were performed. We used the DFT method (B3LYP) with the 6-311++G** basis set implemented in the Gaussian 09 program suite.[37] To treat the solvent molecules explicitly, three DMSO molecules were added to the calculations. The geometric optimization of a metal azide ion pair with three DMSO molecules was carried out, and the frequencies of all normal modes were calculated. As an example, Figure 5B displays the optimized structure of the LiN_3 ion pair with three DMSO molecules. In the optimized structure, the oxygen atoms of DMSO molecules are directly bound to Li^+ ion. Li^+ ion is not along the molecular axis of N_3^- ion, and the angle of Li−N−N in the LiN_3 ion pair is 126°. The optimized structures of other metal ion pairs look similar (see the Supporting Information). Table 4 summarizes the results of quantum chemical calculation of metal azide ion pairs in DMSO. First, the calculated frequencies of the ν_3 mode of N_3^- seem to be overestimated, but the general trend agrees reasonably with the experimental results. Second, the frequency of the $M^{z+}-N_3^-$ stretch mode is correlated with the distance between the metal ion and N_3^- ion. The higher frequency of $M^{z+}-N_3^-$ stretching vibration (or the shorter distance) indicates the strong interaction between metal ion and N_3^- ion. For example, the LiN_3 (or MgN_3^+) ion pair is more strongly bound than the NaN_3 (CaN_3^+) ion pair. In the same way, the distance between metal ion and DMSO molecule is used to estimate the relative strength of the interaction between the metal ion and bound DMSO molecules. For LiN_3 and MgN_3^+ ion pairs, the distance between the metal ion and the oxygen atom of DMSO molecule is shorter when compared with NaN_3 and CaN_3^+ ion pairs. This indicates that the metal ion has a stronger interaction with neighboring DMSO molecules in LiN_3 and MgN_3^+ ion pairs than NaN_3 and CaN_3^+ ion pairs. Thus, the orientational relaxation of LiN_3 and MgN_3^+ ion pairs shows a superstick behavior. Furthermore, $\tau_l/\tau_{rot}^{stick}$ is relatively larger for the MgN_3^+ ion pair than the LiN_3 ion pair because the charge of the Mg^{2+} ion is twice larger than that of Li^+ ion but the distance of $M^{z+}-N_3^-$ is similar. In the case of the MgN_3^+ ion pair, the overall orientational diffusion of the MgN_3^+ ion pair may be accompanied by the strongly bound DMSO molecules.

IV. SUMMARY AND CONCLUDING REMARKS

Azide ion forms contact ion pairs with alkali metal (Li^+ and Na^+) and alkaline earth metal (Mg^{2+} and Ca^{2+}) ions in a polar solvent with a large dielectric constant. Here, we have investigated the metal azide ion pairs in DMSO solutions by FTIR and IR PP spectroscopy as well as quantum chemical calculations. In metal azide ion pairs, the vibrational frequency of azide ion is sensitively varied depending on the countercation and thus individual metal azide ion pairs are spectrally distinguished from free azide ion in the FTIR spectrum. In addition, such spectroscopic properties were utilized to investigate the vibrational population relaxation and orientational relaxation dynamics of individual metal azide ion pairs in DMSO solutions.

The vibrational lifetime of free azide ion was measured to be T_1 = 9.7 ps in DMSO. The vibrational lifetime of azide ion in metal azide ion pairs is relatively longer than that of free azide ion. This is because the metal ion behaves like a thermal insulator by slowing down the intermolecular vibrational energy transfer to the neighboring DMSO molecules. In contrast, the vibrational lifetime of azide ion in the NH_4N_3 ion pair was much shorter than that of free azide ion. In this case, the NH_4^+ ion accepts the vibrational energy from azide ion more efficiently than DMSO molecules and accelerates the population relaxation of azide ion.

Orientational relaxation dynamics, $r(t)$, of free azide ion and metal azide ion pairs in DMSO solutions were well described by a biexponential function. In the case of free azide ions in DMSO solutions with different viscosity, the short time component of $r(t)$ was found to be independent of the solution viscosity, while the long time component was viscosity-dependent. $r(t)$ of metal azide ion pairs in DMSO was significantly dependent on the countercation. $r(t)$ of metal azide ion pairs was analyzed by the wobbling-in-a-cone model and extended Debye−Stokes−Einstein equation. In addition, quantum chemical calculations were carried out to obtain the structural and spectroscopic information on metal azide ion pairs in DMSO solutions. The overall orientational relaxation of free N_3^- ion and the CaN_3^+ ion pair was well described under stick boundary conditions. However, the overall orientational relaxation of LiN_3 and MgN_3^+ ion pairs shows a superstick behavior resulting from the strong interaction between metal ions (Li^+ and Mg^{2+}) and surrounding DMSO molecules.

Rotational dynamics of a small solute molecule whose sizes are comparable with the solvent molecules are sensitively dependent on the detailed structure of the local environments of the solute molecule. This is mainly because rotational

dynamics are dependent on the interaction between the solute and its neighboring solvent molecules. In polar solvents, the rotational dynamics of small ions or dipolar solutes seem to be well described under stick or superstick boundary conditions because ionic or dipolar solute molecules have a relative strong interaction (i.e., ion−dipole or dipole−dipole interaction) with neighboring polar solvent molecules. Such interactions are more important for the solutes whose sizes are smaller than or comparable with the dipolar solvent molecules. Our experimental results can be generally applicable to understand the rotational dynamics of small ionic species in polar solvents.

■ ASSOCIATED CONTENT

Supporting Information

Three figures, showing frequency-resolved IR pump−probe signals obtained with all the sample solutions, vibrational population decay and orientational anisotropy decay of free azide ion in DMSO, and optimized structures of metal azide ion pairs. This material is available free of charge via the Internet at http://pubs.acs.org.

■ AUTHOR INFORMATION

Corresponding Author

*E-mail: spark8@korea.ac.kr.

Notes

The authors declare no competing financial interest.

■ ACKNOWLEDGMENTS

This work was supported by NRF grants (Nos. 20100005020, 20110002122, and 20110020033). This work was also supported by the Human Resources Development of the KETEP grant (No. 20104010100640).

■ REFERENCES

(1) Baldwin, R. L. How Hofmeister Ion Interactions Affect Protein Stability. *Biophys. J.* **1996**, *71*, 2056−2063.
(2) Nostro, P. L.; Ninham, B. W. Hofmeister Phenomena: An Update on Ion Specificity in Biology. *Chem. Rev.* **2012**, *112*, 2286−2322.
(3) Marcus, Y.; Hefter, G. Ion Paring. *Chem. Rev.* **2006**, *106*, 4585−4621.
(4) Park, K.-H.; Choi, S. R.; Choi, J.-H.; Park, S.; Cho, M. Real-Time Probing of Ion Pairing Dynamics with 2DIR Spectroscopy. *ChemPhysChem* **2010**, *11*, 3632−3637.
(5) Lee, K.-K.; Park, K.-H.; Kwon, D.; Choi, J.-H.; Son, H.; Park, S.; Cho, M. Ion-Pairing Dynamics of Li^+ and SCN^- in Dimethylformamide Dolution: Chemical Exchange Two-Dimensional Infrared Spectroscopy. *J. Chem. Phys.* **2011**, *134* (064506), 1−10.
(6) Bian, H. T.; Wen, X. W.; Li, J. B.; Chen, H. L.; Han, S. Z.; Sun, X. Q.; Song, J. A.; Zhuang, W.; Zheng, J. R. Ion Clustering in Aqueous Solutions Probed with Vibrational Energy Transfer. *Proc. Natl. Acad. Sci. U.S.A.* **2011**, *108*, 4737−4742.
(7) Kim, H.; Park, S.; Cho, M. Rotational Dynamics of Thiocyanate Ions in Highly Concentrated Aqueous Solutions. *Phys. Chem. Chem. Phys.* **2012**, *14*, 6233−6240.
(8) Jin, H.; Baker, G. A.; Arzhantsev, S.; Dong, J.; Maroncelli, M. Solvation and Rotational Dynamics of Coumarin 153 in Ionic Liquids: Comparisons to Conventional Solvents. *J. Phys. Chem. B* **2007**, *111*, 7291−7302.
(9) Khara, D. C.; Samanta, A. Rotational Dynamics of Positively and Negatively Charged Solutes in Ionic Liquid and Viscous Molecular Solvent Studied by Time-Resolved Fluorescence Anisotropy Measurements. *Phys. Chem. Chem. Phys.* **2010**, *12*, 7671−7677.
(10) Das, S. K.; Sarkar, M. Rotational Dynamics of Coumarin-153 and 4-Aminophthalimide in 1-Ethyl-3-methylimidazolium Alkylsulfate Ionic Liquids: Effect of Alkyl Chain Length on the Rotational Dynamics. *J. Phys. Chem. B* **2012**, *116*, 194−202.
(11) Zhong, Q.; Baronavski, A. P.; Owrutsky, J. C. Reorientation and Vibrational Energy Relaxation of Pseudohalide Ions Confined in Reverse Micelle Water Pools. *J. Chem. Phys.* **2003**, *119*, 9171−9177.
(12) Son, H.; Haneul, J.; Choi, S. R.; Jung, H. W.; Park, S. Infrared Probing of Equilibrium and Dynamics of Metal-Selenocyanate Ion Pairs in N, N-Dimethylformamide Solutions. *J. Phys. Chem. B* **2012**, *116*, 9152−9159.
(13) Wong, D. B.; Sokolowsky, K. P.; El-Barghouthi, M. I.; Fenn, E. E.; Giammanco, C. H.; Sturlaugson, A. L.; Fayer, M. D. Water Dynamics in Water/DMSO Binary Mixtures. *J. Phys. Chem. B* **2012**, *116*, 5479−5490.
(14) Kumar, P. V.; Maroncelli, M. The Non-Separability of "Dielectric" and "Mechanical" Friction in Molecular Systems: a Simulation Study. *J. Chem. Phys.* **2000**, *112*, 5370−5381.
(15) Dutt, G. B.; Ghanty, T. K. Rotational Diffusion of Coumarins in Electrolyte Solutions: The roles of ion pairs. *J. Phys. Chem. B* **2008**, *107*, 3257−3264.
(16) Park, S.; Fayer, M. D. Hydrogen Bond Dynamics in Aqueous NaBr Solutions. *Proc. Natl. Acad. Sci. U.S.A.* **2007**, *104*, 16731−16738.
(17) Mali, K. S.; Dutt, G. B.; Mukherjee, T. Rotational Diffusion of a Nonpolar and a Dipolar Solute in 1-Butyl-3-Methylimidazolium Hexafluorophosphate and Glycerol: Interplay of Size Effects and Specific Interactions. *J. Chem. Phys.* **2008**, *128* (054504), 1−9.
(18) Gayathri, B. R.; Mannekutla, J. R.; Inamdar, S. R. Rotational Diffusion of Coumarins in Alcohols: A Dielectric Friction Study. *J. Fluoresc.* **2008**, *18*, 943−952.
(19) Le Borgne, C.; Illien, B.; Beignon, M.; Chabanel, M. Ion Association of Alkali and Alkaline Earth Metal Azides in Dimethylsulfoxide. Infrared Spectrometry and Ab Initio Calculations. *Phys. Chem. Chem. Phys.* **1999**, *1*, 4701−4706.
(20) Zhong, Q.; Owrutsky, J. C. Vibrational Energy Relaxation and Reorientation of Azide Ion Pairs in DMSO. *Chem. Phys. Lett.* **2004**, *383*, 176−180.
(21) Sando, G. M.; Dahl, K.; Owrutsky, J. C. Vibrational Relaxation Dynamics of Azide in Ionic and Nonionic Reverse Micelles. *J. Phys. Chem. A* **2004**, *108*, 11209−11217.
(22) Sando, G. M.; Dahl, K.; Owrutsky, J. C. Vibrational Spectroscopy and Dynamics of Azide Ion in Ionic Liquid and Dimethyl Sulfoxide Water Mixtures. *J. Phys. Chem. B* **2007**, *11*, 4901−4909.
(23) Owrutsky, J. C.; Pomfret, M. B.; Barton, D. J.; Kidwell, D. A. Fourier Transform Infrared Spectroscopy of Azide and Cyanate Ion Pairs in AOT Reverse Micelles. *J. Chem. Phys.* **2008**, *129* (024513), 1−10.
(24) Moilanen, D. E.; Levinger, N.; Spry, D. B.; Fayer, M. D. Confinement or the Nature of the Interface? Dynamics of Nanoscopic Water. *J. Am. Chem. Soc.* **2007**, *129*, 14311−14318.
(25) Park, S.; Moilanen, D. E.; Fayer, M. D. Water Dynamics:The Effects of Ions and Nanoconfinement. *J. Phys. Chem. B* **2008**, *102*, 5279−5290.
(26) Lee, H.; Choi, J.-H.; Cho, M. Vibrational Solvatochromism and Electrochromism of Cyanide, Tthiocyanate, and Azide Anions in Water. *Phys. Chem. Chem. Phys.* **2010**, *12*, 12658−12669.
(27) Bagchi, S.; Fried, S. D.; Boxer, S. G. A Solvatochromic Model Calibrates Nitriles' Vibrational Frequencies to Electrostatic Fields. *J. Am. Chem. Soc.* **2012**, *134*, 10373−10376.
(28) Oxtoby, D. W. Vibrational Relaxation in Liquids. *Annu. Rev. Phys. Chem.* **1981**, *32*, 77−101.
(29) Lenchenkov, V.; She, C.; Lian, T. Vibrational Relaxation of CN stretch of Pseudo-Halide Anions (OCN^-, SCN^-, $SeCN^-$) in Polar Solvents. *J. Phys. Chem. B* **2006**, *110*, 19990−19997.
(30) Ohta, K.; Tominaga, K. Vibrational Population Relaxation of Thiocyanate Ion in Polar Solvents Studied by Ultrafast Infrared Spectroscopy. *Chem. Phys. Lett.* **2006**, *429*, 136−140.
(31) Park, S.; Odelius, M.; Gaffney, K. J. Ultrafast Dynamics of Hydrogen Bond Exchange in Aqueous Ionic Solutions. *J. Phys. Chem. B* **2009**, *113*, 7825−7835.

(32) Gaffney, K. J.; Piletic, I. R.; Fayer, M. D. Orientational Relaxation and Vibrational Excitation Transfer in Methanol - Carbon Tetrachloride Solutions. *J. Chem. Phys.* **2003**, *118*, 2270−2278.
(33) Tan, H.-S.; Piletic, I. R.; Fayer, M. D. Orientational Dynamics of Water Confined on a Nanometer Length Scale in Reverse Micelles. *J. Chem. Phys.* **2005**, *122* (174501), 1−9.
(34) Lipari, G.; Szabo, A. Effect of Librational Motion on Fluorescence Depolarization and Nuclear Magnetic Resonance Relaxation in Macromolecules and Membranes. *Biophys. J.* **1980**, *30*, 489−506.
(35) Perrin, F. Mouvement brownien d'un ellipsoide - I. Dispersion Diélectrique Pour des Molécules Ellipsoidales. *J. Phys. Radium* **1934**, *5*, 497−511.
(36) Hu, C.-M.; Zwanzig, R. Rotational Friction Coefficients for Spheroids with the Slipping Boundary Condition. *J. Chem. Phys.* **1974**, *60*, 4354−4357.
(37) Frisch, M. J.; Trucks, G. W.; Schlegel, H. B.; Scuseria, G. E.; Robb, M. A.; Cheeseman, J. R.; Montgomery, J. A., Jr.; Vreven, T.; Kudin, K. N.; Burant, J. C.; et al. *Gaussian 09*, rev. C. 01; Gaussian, Inc.: Wallingford, CT, 2012.
(38) Atkins, P.; Overton, T.; Rourke, J.; Weller, M.; Armstrong, F. *Inorganic Chemistry*, 4th ed.; Oxford University Press: Oxford, U.K., 2006.